Response of intertidal benthic microalgal biofilms to a coupled light-temperature stress: evidence for latitudinal adaptation along the Atlantic coast of Southern Europe.

Martin Laviale, Alexandre Barnett, João Ezequiel, Bernard Lepetit, Silja Frankenbach, Vona Méléder, João Serôdio, Johann Lavaud

▶ **To cite this version:**

Martin Laviale, Alexandre Barnett, João Ezequiel, Bernard Lepetit, Silja Frankenbach, et al.. Response of intertidal benthic microalgal biofilms to a coupled light-temperature stress: evidence for latitudinal adaptation along the Atlantic coast of Southern Europe.. Environmental Microbiology, 2015, pp.3662-3677. 10.1111/1462-2920.12728 . hal-01097838

HAL Id: hal-01097838
https://hal.science/hal-01097838v1

Submitted on 9 Jan 2015

HAL is a multi-disciplinary open access archive for the deposit and dissemination of scientific research documents, whether they are published or not. The documents may come from teaching and research institutions in France or abroad, or from public or private research centers.

L'archive ouverte pluridisciplinaire **HAL**, est destinée au dépôt et à la diffusion de documents scientifiques de niveau recherche, publiés ou non, émanant des établissements d'enseignement et de recherche français ou étrangers, des laboratoires publics ou privés.

Response of intertidal benthic microalgal biofilms to a coupled light-temperature stress: evidence for latitudinal adaptation along the Atlantic coast of Southern Europe.

Martin Laviale,[1*] Alexandre Barnett,[2] João Ezequiel,[1] Bernard Lepetit,[2#] Silja Frankenbach,[1] Vona Méléder,[2,3] João Serôdio[1] and Johann Lavaud[2]

[1] Departamento de Biologia and CESAM – Centro de Estudos do Ambiente e do Mar, Universidade de Aveiro, Campus de Santiago, 3810-193 Aveiro, Portugal

[2] UMRi7266 LIENSs 'Littoral, Environnement et Sociétés', CNRS/Université de La Rochelle, Institut du Littoral et de l'Environnement, 2 rue Olympe de Gouges, 17000 La Rochelle, France.

[3] LUNAM Université, Université de Nantes, EA 21 60 MMS 'Mer, Molécules, Santé', 2 rue de la Houssinière, BP 92 208, 44322, Nantes Cedex 3, France

Current address: Plant Ecophysiology, Department of Biology, University of Konstanz, Universitätsstraße 10, 78457 Konstanz, Germany

* Corresponding author:

Departamento de Biologia and CESAM – Centro de Estudos do Ambiente e do Mar, Universidade de Aveiro, Campus de Santiago, 3810-193 Aveiro, Portugal

Phone: +351 234 370 968; Fax: +351 234 372 587; E-mail: martin.laviale.bio@gmail.com

Running title: microphytobenthos response to light-temperature stress

Summary:

Although estuarine microphytobenthos (MPB) is frequently exposed to excessive light and temperature conditions, little is known on their interactive effects on MPB primary productivity. Laboratory and *in situ* experiments were combined to investigate the short-term joint effects of high light (HL) and high temperature (37°C *vs.* 27°C) on the operating efficiency of photoprotective processes (vertical migration *vs.* non-photochemical quenching: NPQ) exhibited by natural benthic diatom communities from two intertidal flats in France (FR) and Portugal (PT). A clear latitudinal pattern was observed, with PT biofilms being more resistant to HL stress, regardless the effect of temperature, and displaying a lower relative contribution of vertical migration to photoprotection and a stronger NPQ *in situ*. However, higher temperature leads to comparable effects, with photoinhibition increasing to about 3-times (i.e. from 3 to 10 % and from 8 to 22 % in PT and FR sites, respectively). By using a number of methodological novelties in MPB research (lipid peroxidation quantification, Lhcx proteins immunodetection), this study brings a physiological basis to the previously reported depression of MPB photosynthetic productivity in summer. They emphasize the joint role of temperature and light in limiting, at least transiently (i.e. during emersion), MPB photosynthetic activity *in situ*.

Introduction

Estuarine tidal flats are one of the most productive ecosystems on Earth, largely owing to the photosynthetic productivity of benthic microalgae communities, or microphytobenthos (MPB) (Underwood and Kromkamp, 1999). MPB communities are often dominated by motile pennate diatoms (Haubois *et al.*, 2005; Méléder *et al.*, 2007; Ribeiro *et al.*, 2013). In fine sediment habitats, they undergo rhythmic vertical migration patterns in the upper layers of the sediment following tidal/dial cycles (Saburova and Polikarpov, 2003; Consalvey *et al.*, 2004; Coelho *et al.*, 2011). During daylight emersion, the upward migration of cells results in the formation of transient photosynthetic biofilms which are thus periodically exposed to variable and extreme environmental conditions, due to the complex interplay of timing of tidal exposure and weather conditions (Admiraal 1984; Paterson and Hagerthey, 2001). Excessive light exposure generates intra-cellular oxidative stress (Roncarati *et al.*, 2008; Waring *et al.*, 2010) which can lower photosynthetic efficiency (i.e. photoinhibition; Wu *et al.*, 2012; Cartaxana *et al.*, 2013) and ultimately community-level primary productivity (Blanchard *et al.*, 1996; Guarini *et al.*, 2006). Furthermore, benthic diatom's photosynthesis often operates under the combined action of high light and other potentially stressful environmental factors such as extreme temperature (Blanchard *et al.*, 1997; Serôdio and Catarino, 1999). Although photosynthesis is known to be highly sensitive to temperature (Mathur *et al.*, 2014), effects of high temperature on MPB productivity, either alone or in combination with excess light have received little attention (Grant, 1986; Vieira *et al.*, 2013 and references therein). However, recent results showed implications on both dial and seasonal scales (Hancke *et al.*, 2014). On a longer term perspective, the cumulative effects of light and temperature could be relevant as well, as climate change is expected to influence not only average values but also the frequency and the intensity of extreme events such as heat waves (Schär *et al.*, 2004; Stott *et al.*, 2004; Solomon *et al.*, 2007).

The actual photoinhibitory effects depend on the photoadaptive strategy of the diatoms of MPB, i.e. the operating efficiency of a range of mechanisms which include 'behavioural' and 'physiological' photoprotective processes (Barnett *et al.*, 2014). The 'behavioural photoprotection' consists of a strong negative phototaxis resulting in downward migration under supersaturating light intensities (Kromkamp *et al.*, 1998; Perkins *et al.*, 2010; Cartaxana *et al.*, 2011; Serôdio *et al.*, 2012). The vertical migration of cells within the steep light gradient of the sediment photic zone (Paterson and Hagerthey, 2001; Cartaxana *et al.*, 2011) has been hypothesized to allow for the optimization of light harvesting and the avoidance of excess light (Admiraal, 1984). Strong evidence for a photoprotective role of vertical migration was provided by the use of the diatom motility inhibitor Latrunculin A (Lat A) on undisturbed biofilms (Perkins *et al.*, 2010; Cartaxana *et al.*, 2011; Serôdio *et al.*, 2012). 'Physiological photoprotection' mainly includes the excess energy-dissipative non-photochemical quenching of chlorophyll (Chl) *a* fluorescence (NPQ). NPQ is mainly controlled by the presence of the xanthophyll pigment diatoxanthin (DT) and of Lhcx proteins in the light-harvesting complexes of photosystem II (PSII) (Depauw *et al.*, 2012; Lepetit *et al.*, 2012, 2013; Lavaud and Goss, 2014). In diatoms, DT is produced by the (dark/low light) reversible light-dependent conversion of the xanthophyll diadinoxanthin (DD) in the so called xanthophyll cycle (XC) (Goss and Jakob, 2010). Besides its involvement in NPQ, it seems to have another function as antioxidant (Lepetit *et al.*, 2010).

Despite the crucial role of NPQ and XC in the photoprotective response of diatoms to excessive fluctuating light regimes, especially in field situations (Brunet *et al.*, 2010; Lavaud and Lepetit, 2013; Lavaud and Goss, 2014), they have only scarcely been studied in MPB. They show a relation to diurnal and tidal cycles, season, latitude (Serôdio *et al.*, 2005; van Leeuwe *et al.*, 2008; Chevalier *et al.*, 2010), to vertical position of diatoms within the sediment (Jesus *et al.*, 2009; Cartaxana *et al.*, 2011) or along the intertidal elevation gradient

(Jesus *et al.*, 2009), with significant differences between the main growth forms (i.e. epipelic and epipsammic: Cartaxana *et al.*, 2011; Barnett *et al.*, 2014). As for the implication of Lhcx proteins in diatom NPQ, its characterization has been limited to few model species (Bailleul *et al.* 2010; Zhu *et al.*, 2010). Lhcx1 is involved probably at least by binding DT (Bailleul *et al.*, 2010; Büchel, 2014). It is present at low light and its transcript level/synthesis is slightly enhanced under high light (HL) (Bailleul *et al.*, 2010; Wu *et al.*, 2012; Lepetit *et al.*, 2013). While the transcript levels/synthesis of other examined isoforms (i.e. Lhcx2, Lhcx3, Lhcx6) strongly increase during HL (Zhu *et al.*, 2010; Lepetit *et al.*, 2013) and temperature stress (for Lhcx6; Wu *et al.*, 2012), their exact physiological role remains unknown, although Lhcx3 and Lhcx6 are suspected to be involved in the binding of *de novo* synthesized DT and/or the sustain part of NPQ (i.e. qI) during a prolonged HL stress (Zhu *et al.*, 2010; Lepetit *et al.*, 2013).

This work intended to study the combined effects of high light (HL) and high temperature on the photophysiology of intertidal diatom-dominated MPB communities. Light stress-recovery experiments (LSRE) were performed to distinguish physiological photoprotection efficiency from photoinhibitory effects, and to quantify behavioural photoprotection (Serôdio *et al.*, 2012). Until now, these processes have been characterized only to the extent of chlorophyll fluorescence measurements and XC pigments analysis. The present study combines chlorophyll fluorescence imaging, pigment analysis and for the first time on intact biofilms, lipid peroxidation quantification and immunodetection of Lhcx proteins. LSRE were performed on MPB from two locations in France and Portugal with different solar exposure and temperature regimes, likely to support the establishment of diatom communities with contrasting photo- and thermo-adaptive strategies. Moreover, the potential role of temperature in modulating the HL-induced stress was investigated by carrying out LSRE at two experimental temperature conditions (‘optimal’ *vs*. high temperature). In parallel, the

117 estimated photosynthetic and protective indices were further compared with field situation at
118 the two sites during a typical summer diurnal emersion.

119

Results

Environmental conditions, in situ *photosynthetic activity and taxonomic composition of microphytobenthos in PT and FR sites*

Environmental conditions and MPB photosynthetic activity were assessed during typical summer diurnal emersion at both Portuguese (PT) and French (FR) intertidal flats. The Photosynthetic Active Radiation (PAR) reached its daily maximum (2000 µmol photons m^{-2} s^{-1}) at both sites (Fig. 1A-B) with a comparable light dose over the emersion (~19 to 23 mol photons m^{-2}, Table S1). Temperature was higher at PT site (Fig. 1A-B). Average temperatures at the sediment surface were 37.5°C and 28.8°C for PT and FR sites, respectively. Temperature decreased with sediment depth with a stronger effect in PT site (-7°C and -6°C in the first 0.5 cm for PT and FR sites, respectively: Table S1, Fig. 1A-B).

At the beginning of emersion, the effective PSII quantum yield (ΦPSII) was close to its optimum at both sites (~ 0.70: Fig. 1C-D, open squares). It decreased/increased opposite to the PAR evolution over the emersion period, reaching values as low as ~ 0.40. The maximal non-photochemical quenching of Chl *a* fluorescence (NPQ_{max}) was about 4-5 at PT site and lower than 1 at FR site at the beginning of emersion (Fig. 1C-D, closed circles). It decreased continuously at PT site to reach values around 3 at the end of the emersion, while it covaried with PAR at FR site, reaching a maximum value of about 6 (matching the sudden increase in PAR level) and values of 3-4 at the end of the emersion.

At both sites, MBP communities were dominated by epipelic (i.e. motile) benthic diatoms of the genus *Navicula* (Table S2). *Navicula phyllepta* sensu lato (Vanelslander *et al.,* 2009) was the dominant species at PT site (relative abundance: 44 %) while FR site was co-dominated by *N. spartinetensis* (33 %) and *N. phyllepta* s.l. (28 %).

Comparison between in situ *and experimental conditions*

The two temperature treatments used for the laboratory experiments during the LSREs were 27.4 ± 1.2°C and 37.3 ± 0.7°C (thereafter named 27°C and 37°C temperature treatments, respectively), which was close to the average temperatures monitored at the sediment surface for both sites (see above and Table S1). The light exposure of 3 h of 1200 µmol photons m^{-2} s^{-1} represented a light dose of 12.96 mol photons m^{-2} (Serôdio *et al.*, 2012). This light dose was reached after 2 h 53 min and 3 h 34 min in PT and FR sites, respectively (Table S1).

LSRE-induced photoinhibition and NPQ in sediment from FR site

ΦPSII remained constant in samples maintained under LL throughout the experiment (0.66 ± 0.02, Fig. 2). In comparison, samples exposed to HL exhibited dramatic changes over time (time: $P < 0.001$, see Table S3a for detailed statistical outputs). After 3h HL, ΦPSII decreased down to values between 0.13 ± 0.03 (37°C +Lat A) and 0.34 ± 0.02 (27°C Ctrl). It increased during LL recovery but did not reach back its initial level (0.46 ± 0.05 (37°C +Lat A) and 0.61 ± 0.01 (27°C Ctrl). The differences observed between temperature and chemical treatments were significant (temperature: $P < 0.001$; chemical: $P < 0.01$; Table S3a), and they both increased with time (time × temperature: $P < 0.001$; time × chemical: $P < 0.05$; Table S3a). Similarly, NPQ of samples maintained under LL remained constant (0.38 ± 0.04, Fig. 3) and changed over time according to light (time: $P < 0.001$, Table S3b): it increased under HL (between 4.4 ± 0.5 and 3.4 ± 0.4 from 37°C +Lat A and 27°C Ctrl treatments, respectively) but only partially relaxed during the subsequent 15 min LL incubation (between 1.9 ± 0.1 and 1.1 ± 0.1; Fig. 3). The effect of temperature was highly significant (temperature: $P < 0.001$, Table S3b) and the observed differences increased with time (time × temperature: $P < 0.001$; Table S3b). In comparison, the effect of lat A was less significant (chemical: $P < 0.05$ and time × temperature: $P = 0.11$; Table S3b).

LSRE-induced allomerization of Chl a *and xanthophyll cycle in sediment from FR site*

All samples exhibited typical diatom pigment signatures, including Chl *a*, Chls *c*, fucoxanthin, the carotenoid ß, ß carotene (data not shown) and the xanthophyll cycle pigments DD and DT. The allomer form of Chl *a* (Chl *a*-allo) accumulated during the LSRE as illustrated by the Chl *a* allomerization molar ratio (AR= Chl *a*-allo / total Chl *a* × 100, Fig. 4A). AR increased ~ 2-fold under HL and remained stable thereafter (time: $P < 0.001$; Table S3c). No significant changes were observed with temperature (temperature: $P = 0.48$; Table S3c), whereas AR was significantly higher in +Lat A samples than in Ctrl (chemical: $P < 0.01$; Table S3c), with mean maximum values of 11.9 ± 5.0% and 8.4 ± 2.1%, respectively (Fig. S1). AR did not significantly change in samples maintained in LL during 3 h (5.9 ± 2.7% on average).

The pool of DD+DT (in mol. 100 mol Chl a^{-1}) increased ~ 3-fold under HL and remained stable during the LL recovery (Fig. 4B, time: $P < 0.001$; Table S3d). Overall, it reached higher values at 37°C than at 27°C (temperature: $P < 0.01$; Table S3d) but it was comparable in Ctrl and +Lat A samples ($P = 0.58$; Table S3d). At 37°C, DD+DT increased even in the samples maintained under LL for 3 h (from 15.0 ± 4.0 to 23.8 ± 6.6 mol. 100 mol Chl a^{-1}, Tukey HSD: $P < 0.05$, Fig. S2). DD de-epoxidation (DES = DT / DD+DT × 100) correlated well with light whatever the temperature in both Ctrl and Lat A-treated samples ($P < 0.001$) (Fig. 4C-D). DES increased under HL and decreased during LL recovery while it remained stable in samples maintained in LL for 3 h (14.0 ± 3.2% on average) (Fig. S3). DES was significantly higher in +Lat A samples than in Ctrl ones (chemical: $P < 0.001$; Table S3d), and at 37°C than at 27°C (temperature: $P < 0.001$; Table S3d) with maxima of 67.2 ± 7.5% and 33.8 ± 7.5% at 37 °C and 27 °C, respectively, in +Lat A samples (Fig. S3). DES recovered much faster at 27°C than at 37°C, especially for Ctrl samples. In contrast to AR and the DD+DT pool, interaction between time and temperature was significant for DES (time ×

195 temperature: $P < 0.001$; Table S3d). Moreover, NPQ and DES were significantly positively
196 correlated according to the chemical treatment (Ctrl/+Lat A), *i.e.* the slope of the NPQ *vs*.
197 DES linear regression was 2.5 lower in +Lat A samples (Fig. S4) while for both treatments
198 the origin of the regression was similar and non-nul (Ctrl: 17.6 ± 0.4; +Lat A: 16.4 ± 0.4), i.e.
199 some DT was synthesized without NPQ development.
200
201 *LSRE-induced Lhcx synthesis in sediment from FR site*
202 The anti-FCP6 (i.e. Lhcx1) revealed a clear Lhcx isoform in FR samples (Fig. 5A). Its size of
203 about 24 kDa was slightly higher than the one of Lhcx 3 in *Phaeodactylum tricornutum* and
204 its amount increased after 3 h HL exposure especially in +Lat A samples. Interestingly, *N.*
205 *phyllepta* s.l., the dominant species of the MPB assemblage, showed an Lhcx pattern similar
206 to *P. tricornutum* so that three isoforms (Lhcx1, Lhcx2 and Lhcx3) could be identified. The
207 anti-Lhcx6 from *Thalassiosira pseudonana* revealed two Lhcx isoforms in FR samples, the
208 size of which was different from Lhcx6 and was neither present in HL exposed *P. tricornutum*
209 cells (Fig. 5B). *N. phyllepta* showed two isoforms, one which size was slightly higher than
210 Lhcx6 and the other one with a similar size to the 33-50 kDa isoform from FR samples. With
211 such size, this isoform could be a hypothetic Lhcx dimer (given that the available sizes of
212 Lhcx monomers deduced from the genomes of *P. tricornutum*, *T. pseudonana* and
213 *Fragilariopsis cylindrus* range between 21 and 29 kDa) but different than in *P. tricornutum*.
214 The 17-23 kDa isoform showed a size similar to Lhcx 1 in *P. tricornutum* and *N. phyllepta*
215 (see Fig. 5A). Interestingly, the two isoforms reacted to light, temperature and Lat A in
216 different ways: while the 17-23 kDa isoform appeared not to react to any of the treatments,
217 the 33-50 kDa isoform positively reacted to HL and 37°C with an effect enhanced by Lat A at
218 37°C (Fig. 5C).
219

220 *LSRE-induced lipid peroxidation in sediment from FR site*

221 Common markers of membrane lipid peroxidation (TBARS-thiobarbituric acide reactive
222 substances) were quantified. In Lat A treated samples, TBARS content normalized to the
223 surface microphytobenthos biomass (I_{diat} biomass index) did not change significantly over
224 time and was not significantly affected by chemical or temperature treatments (P = 0.71,
225 0.99 and 0.19, respectively; Table S3f), exhibiting a mean value of 1.19 ± 0.29 10^{-6} nmol eq
226 MDA mL^{-1} (Fig. 6).

227

228 *Comparison between FR and PT sites: NPQ, photoinhibition, lipid peroxidation and Lhcx.*

229 ΦPSII and NPQ measured on PT samples at T0 (0.67 ± 0.02 and 0.40 ± 0.05, respectively)
230 were comparable to the one measured on FR ones (Fig.2 and 3: 0.66 ± 0.01 and 0.39 ± 0.01,
231 respectively), and they exhibited the same general trend under HL stress. However, PT
232 samples were less affected by the HL treatment, as ΦPSII recovered faster under LL (site: P <
233 0.001, Table S4a), regardless of temperature or Lat A application (Fig. 7A). Moreover, NPQ
234 did not relax entirely, but the level of this sustained NPQ was lower than in FR samples (site:
235 P < 0.01, Table S4b), although post-hoc multiple comparison tests did not show any statistical
236 differences between sites (Tukey HSD: P > 0.05; Fig. 7B).

237 For each site and temperature, the extent of photoinhibition and the contribution of vertical
238 migration to the overall photoprotection capacity of MPB were estimated as in Serôdio *et al.*
239 (2012) (Table 1). Photoinhibition was higher in FR than PT site but it increased similarly (~3
240 fold) with temperature. The contribution of vertical migration to photoprotection remained
241 below 15 % but was always lower in PT biofilms (< 5%).

242 In Lat A treated samples, TBARS content normalized to surface biomass did not change
243 significantly at PT site whatever the temperature (Fig. S5). Mean value was 3.26 ± 0.66 10^{-6}
244 nmol eq MDA mL^{-1}, which was significantly higher than for FR samples (t-test: P < 0.001).

While the anti-FCP6 (i.e. Lhcx1) revealed two clear Lhcx isoforms in PT samples (Fig. 8), the anti-Lhcx6 did not bring any signal probably due to its unspecificity as regards to the species composing the microphytobenthic community of PT site. Their respective size were close with one at about 23 kDa, the size of Lhcx 3 in *P. tricornutum* and *N. phyllepta*, and the other one slightly higher (about 24 kDa) which was also present in FR samples (Fig. 5A). Both isoforms (although the 24 kDa reacted in a stronger way) were enhanced after 3 h of HL exposure as well as by the higher temperature; this effect was increased by the addition of Lat A. Interestingly, at 27°C, the 24 kDa isoform was not present under LL and HL exposure, it appeared with the addition of Lat A solely (LL 27°C +) and its content was increased by HL exposure (HL 27°C +). Similarly, the 23 kDa isoform positively reacted to Lat A to a level even similar to HL exposure without Lat A (compare 27°C LL+ and 27°C HL-).

Discussion

In this study, higher temperature significantly increased photoinhibition susceptibility of epipelic MPB biofilm. Communities from the Portuguese (PT) site were clearly more resistant to a coupled high light-temperature stress, in comparison to biofilms from the French (FR) site. At both site, photoprotection was based on the interplay between physiological (NPQ, DT and Lhcx proteins) and behavioural (vertical motility) response, nevertheless PT biofilms displayed a lower relative contribution of vertical migration and a stronger NPQ. The apparent latitudinal pattern observed at the community level ('MPB biofilm') might be driven by the individual response of the respective dominant diatom species/ecotypes in each site. These different aspects are discussed below.

Evidence for a latitudinal adaptation in the response of epipelic MPB to a coupled light-temperature stress

Our results suggest that PT MPB communities were adapted to a higher light and/or temperature environment than FR ones. Overall, PT samples were more resistant than FR ones to HL stress, regardless the effect of temperature. At 27°C, PT control samples recovered almost entirely from HL exposure (97 %), and photoinhibition increased only from 3 to 10 % at 37°C. This trend was also obvious *in situ*: the time course and level of ΦPSII were comparable between sites despite the potentially more stressful conditions at PT site (similar light conditions but 8-9°C higher average surface temperature). One of the reasons for this differential latitudinal adaptation might lie in the photoprotective strategies the two MPB communities exhibited. PT MPB communities showed higher NPQ_{max} average values, an indication of a strong(er) physiological photoprotective response (Serôdio *et al.*, 2005). PT NPQ_{max} was already high right from the beginning of the emersion although light intensity was still moderate and it remained relatively stable along the emersion. Consequently, vertical

migration contributed less to the overall photoprotection capacity (< 5 %) in comparison to FR biofilms. FR NPQ_{max} tended to follow the fluctuations of light intensity along the emersion which would be in agreement with a more dynamics MPB response, regarding both motility and physiology. Only few studies have examined the link between seasonal and/or latitudinal photoacclimation and the coupling between behavioural and physiological photoprotection in MPB communities. A similar increase of migration contribution was reported for communities acclimated to lower irradiances (i.e. seasonal acclimation: Serôdio *et al.*, 2012). Another study provided evidence for the differential role of migration *vs*. XC along a latitudinal gradient (Ireland, UK and Portugal), although the role of sediment type (i.e. mud *vs*. sand) could not be ruled out (van Leeuwe *et al.*, 2008).

In contrast, the contribution of thermal adaptation is difficult to ascertain. Although PT samples were more resistant and resilient, higher temperature leads to comparable effects: photoinhibition increased to about 3-times (i.e. from 3 to 10 % and from 8 to 22 %, in PT and FR sites, respectively) and lipid peroxidation was comparable. The pattern of the detected Lhcx isoforms was also similar, although no quantification was possible. Average surface and -0.5 cm temperature conditions experienced by the FR and PT communities were clearly different. The fact that this difference was lower than the observed amplitude over an emersion could explain the apparent lack of temperature latitudinal pattern. This is in agreement with other comparative studies on short-term (i.e. over few hours) temperature effects on MPB photosynthesis (Grant, 1986; Blanchard *et al.*, 1997; Hancke and Glud, 2004). Instead, the different average temperature conditions at PT and FR sites recorded in this study, which are representative of typical summer conditions in these areas (Guarini *et al.*, 1997; Lillebo *et al.*, 2010), might have played a role on a longer time scale. As temperature and light adaptations rely on similar strategies (Davison, 1991; this study, see below), it is likely that the difference in average temperatures influenced the susceptibility of

MPB to photoinhibition, directly and/or via its photoacclimation status, together with e.g. daily light dose, day length and/or UV exposure.

The latitudinal pattern in ecophysiological characteristics observed at the community level coincided with a shift in the diatom species composition. Although it is difficult to separate 'community' response from 'individual species' response within the biofilm, it is possible that the observed responses at each site were driven by the few dominant species (representing c.a. 50% of the total abundance). The two dominant species, *N. phyllepta* s.l. and N. *spartinetensis*, are known to be widespread along the European Atlantic and Northwestern coasts (Vanelslander *et al*., 2009; Witkowski *et al*., 2012). Epipelic diatoms generally exhibit a low NPQ, in comparison to non-motile ones (Barnett *et al.*, 2014). This does not preclude the existence of interspecific variability between organisms sharing the same life style, considering both behavioural (Underwood *et al.*, 2005; Du *et al.*, 2010, 2012) and physiological photoprotective mechanisms (Barnett *et al.*, 2014). Furthermore, the occurrence of *N. phyllepta* s.l. at both sites can be explained by the pseudocryptic feature of this taxonomic group. It comprises different closely related species morphologically indistinguishable but exhibiting important ecophysiological differences and environmental preferences (Vanelslander *et al*., 2009). To which extent the differences observed between PT and FR sites (i.e. stronger NPQ_{max} in PT assemblage regardless of the stress treatment; different Lhcx patterns) can be explained by the differential relative abundances of *N. phyllepta* s.l. vs. *N. spartinetensis* and/or pseudopcryptic species or ecotypes of *N. phyllepta* s.l is a question that remains to be answered.

Higher temperature increases photoinhibition susceptibility in epipelic MPB

To our knowledge, this is the first study which shows that on intact migratory MPB biofilms high temperature and HL acts synergistically in decreasing photosynthesis, a feature so far

reported only for individual species (Salleh and McMinn, 2011). Other works have shown that temperature alone impacts photosynthesis in benthic diatoms, in monospecific cultures (Morris and Kromkamp, 2003; Yun *et al.*, 2010), MPB suspensions (Blanchard *et al.*, 1997), and intact MPB biofilms (Vieira *et al.*, 2013). In conditions where photosynthesis is light-saturated, benthic diatom photosynthesis can respond to a transient temperature increase if it remains within a 25-35°C range. The high temperature used here (37.3 ± 0.7°C) falls slightly outside this range, a situation likely to occur regularly *in situ* in summer, as confirmed by our field data.

In situ measurements showed that ΦPSII correlated well with irradiance during the emersion period. During LSRE, a strong decrease was also observed after 3 h of HL exposure. Although the applied light dose was lower than *in situ*, our results show that it was strong enough to induce photoinhibition at the community level. The incomplete recovery of ΦPSII after 15 min LL coincided with a sustained phase of NPQ which was induced during the prolonged HL exposure. This can be partly attributed to photoinhibition and illustrates the physiological response to harsh stress (Zhu *et al.*, 2010; Wu *et al.*, 2012; Lavaud and Lepetit, 2013). At optimal temperature (27°C; see Blanchard *et al.*, 1997 and Experimental procedures section), photoinhibition remained below 20 %, which is consistent with a previous study using a similar experimental approach (Serôdio *et al.*, 2012). Photoinhibitory effects may be attributed to the progressive accumulation of reactive oxygen species (ROS, Roncarati *et al.*, 2008; Waring *et al.*, 2010), as evidenced by the increase of AR at the end of LSRE. Indeed, ROS have been shown to be directly involved in Chl *a* allomerization (Hynninen *et al.*, 2010 and references therein). This is also consistent with the accumulation of Chl *a* allomers in response to oxidative stress in the diatom *P. tricornutum* (Cid *et al.*, 1995). When superimposed to HL stress, significantly increased photoinhibition (c.a. 3-times increase in the controls from 27 to 37°C) which is not surprising as PSII is the most thermosensitive

component of the photosynthetic apparatus (Mathur *et al.*, 2014). Nevertheless, the amount of MDA and other aldehydes (TBARS) were not affected, suggesting that antioxidant activities were sufficient to prevent from substantial ROS-mediated membrane damage during the 3 h stress exposure, even when migration was inhibited. In such short-term experiments (i.e. < 24 h), it seems that only stronger oxidative stress such as UV- or herbicides-induced leads to noticeable lipoperoxidation (Rijstenbil, 2005; Wang *et al.*, 2011).

New evidences on the interplay between behavioural and physiological response to light-temperature stress in epipelic microphytobenthos

In response to HL alone, diatoms which were free to move (i.e. in the controls) could reach deeper layers of sediment with lower light conditions, potentially closer to their photosynthetic optimum (Kromkamp *et al.*, 1998). This downward migration contributed to a reduction of the deleterious effects of HL observed in Lat A treated samples (i.e. immobilized cells at the surface of sediment) such as an enhanced accumulation of Chl *a* allomers and a slower ΦPSII recovery. Our results are in agreement with previous works using Lat A on natural biofilms (Perkins *et al.*, 2010; Serôdio *et al.*, 2012). Similarly, the motile diatoms could reach a depth with lower and more stable temperature, as shown by the *in situ* temperature depth profiles monitored here. Nevertheless, our measurements were not refined enough to conclude about the steepness of the vertical temperature gradient in muddy sediment, as for light (Paterson and Hagerthey, 2001; Cartaxana *et al.*, 2011). Additionally, high temperature alone is known to directly affect the motility of MPB diatoms, i.e. over 35°C cell motility significantly drops-down (Cohn *et al.*, 2003; Du *et al.*, 2012). Such feature might partly explain the stronger photoinhibition observed at 37°C in Lat A free samples, together with a direct impact of temperature on physiological mechanisms.

NPQ developed in the same range of mean values (i.e. 3-4) *in situ* than during LSRE with HL stress alone. Concomitantly, the DD+DT pool size as well as DES increased. DT synthesis was based not only on DD de-epoxidation (as illustrated by DES) but also by additional DT *de novo* synthesis (Lavaud and Lepetit, 2013; Lepetit et al., 2013) which enlightened the high level of stress the cells were exposed to. Whatever the source, additional DT provides higher physiological photoprotection via higher NPQ and/or via higher prevention of oxidative lipid peroxidation (Lepetit et al., 2010; Lavaud and Lepetit, 2013). DT synthesis (DD+DT and DES) is enhanced by the high temperature stress alone (Salleh and McMinn, 2011), and this effect was even stronger in conditions of a coupled HL and high temperature stress. Specifically, DD+DT and DES showed a slower recovery which could represent a feed-back reaction (i.e. related to HL/high temperature impairment of the Calvin cycle activity, Mathur *et al.*, 2014) for the maintenance of a photoprotection capacity to cope with prolonged stressful temperature conditions, even under LL (Lavaud and Lepetit, 2013; Lepetit *et al.*, 2013). When the diatom motility was inhibited by Lat A, DES significantly increased independently of the temperature, and its recovery was slower. This was apparently not due to a higher DT *de novo* synthesis as illustrated by the similar DD+DT pool size with and without Lat A. Higher DT synthesis in presence of Lat A had no significant effect on NPQ, except for its increased sustainability when in conjunction with high temperature. Higher sustained NPQ (i.e. qI) is known to be related with both sustained DT and photoinhibition in conditions of a strong stress (Lavaud and Lepetit, 2013; Lepetit et al., 2013). As a consequence, the DT quenching efficiency (i.e. the slope of the NPQ-DT relationship) was lower in presence of Lat A, likely due to the differential involvement of DT molecules in NPQ (Lavaud and Lepetit, 2013): in presence of Lat A, the additional DT molecules instead most probably acted as ROS scavengers in prevention of lipid peroxidation (Lepetit *et al.*, 2010) arguing for a pronounced stress (i.e. HL + hight temperature + inhibition of motility) level.

406 Although, as expected, the Lhcx pattern in sediment samples was not as clear as the one of
407 monocultures of *N. phyllepta*, one of the dominant species common to the FR and PT MPB
408 communities, the confirmation of the presence of some of the known isoforms was possible.
409 While an isoform with a similar size than Lhcx1 apparently did not react to any of the
410 treatments, we found that the synthesis of two isoforms were enhanced by HL, high
411 temperature and Lat A: one isoform with a size similar to Lhcx3, and one isoform with the
412 size of a dimer which especially positively reacted to high temperature and Lat A treatment.
413 Interestingly, these two isoforms were also present in *N. phyllepta*. A third isoform (of about
414 24 kDa), which was not detected in *N. phyllepta*, was synthetized in all treatments. Based on
415 our knowledge of the synthesis and roles of Lhcx proteins during prolonged stress, it is
416 reasonable to argue that these isoforms participated, at least in part, to the above described
417 NPQ and XC patterns during the coupled HL and high temperature stress. Interestingly, the
418 Lhcx3 and 24 kDa isoforms strongly reacted to Lat A out of any stress and to a level
419 comparable to HL stress. It suggests that the inhibition of motility might generate a strong
420 preventive physiological answer in diatom cells blocked at the surface of sediment (which can
421 occur *in situ* during sediment desiccation events for instance), an additional hint that
422 physiological and behavioural photoprotection are closely related in epipelic diatoms. This
423 compensation, together with a stronger NPQ induction and XC activity, was nevertheless not
424 strong enough to prevent immobilized cells from additional photoinhibition, as ΦPSII
425 recovery was always lower in Lat A treated samples than in migratory biofilms.
426
427
428 *Conclusions and perspectives*
429 By using a number of methodological novelties in MPB research (a new cryo-sampling
430 method, lipid peroxidation markers for photooxidative stress-TBARS, photosynthetic protein

markers for physiological protection-Lhcx), the present study clearly strengthens the previous statement of a coupled and complementary action of physiological and behavioural processes in protecting the photosynthetic activity of MPB diatoms in stressful environmental conditions (Perkins et al., 2010, Cartaxana et al., 2011; Serôdio et al., 2012). Moreover, our results bring a physiological basis to the previously reported depression of MPB photosynthetic productivity in summer (Guarini et al., 1997). They emphasize the joint role of temperature and light in limiting, at least transiently (i.e. during emersion), the photosynthetic activity of MPB biofilm *in situ*. They confirm that high temperature, together with high light, is an important environmental driver which supports seasonal, spatial and potentially latitudinal MPB biodiversity and biomass distribution at the scale of intertidal mudflats along the Atlantic coast of Southern Europe (Guarini et al., 1997; Brito et al., 2013).

Moreover, temperature being expected to increase due to global change (Solomon *et al.*, 2007), further longer-term experiments are required in order to question its importance in modulating MPB photosynthetic activity. Our results support previous works suggesting that MPB gross photosynthesis will most probably not be affected by a small increase (even if significant, i.e. +1°C to +4°C for the most extreme previsions; Solomon *et al*., 2007) of average temperature (Vieira *et al.*, 2013; Hancke *et al.*, 2014). However, it does not preclude a potential change in the community structure, as observed for associated invertebrate assemblages (Hicks *et al.*, 2011), which might be of importance in driving the whole community response as reported here. Further experiments should rather focus on the cumulative effects of successive extreme events such as heat waves experienced during spring/summer (Schär *et al*., 2004; Stott *et al*., 2004), with an emphasis on the 'species/individual' *vs*. 'community/biofilm' response.

Experimental procedures

Study areas and experimental design

Two intertidal mudflats were sampled along the Atlantic Coast of Southern Europe, in France and Portugal (FR and PT sites, respectively): a macrotidal one in the Baie de l'Aiguillon near Esnandes (FR, 46°15.36'N, 1°8,55'W) and a mesotidal estuary in the Ria de Aveiro near Vista Alegre (PT, 40°35' N, 8°41' W). Both sites are composed of fine muddy sediments (dominant particle size < 63 µm) and are known to be colonized by epipelic diatom-dominated MPB throughout the year (Haubois *et al*., 2005; Serôdio *et al.*, 2012, respectively).

All experiments were performed consecutively in early summer (weeks 26-27, June-July 2012). For each site, natural migratory MPB was studied *in situ* over one diurnal emersion period. In parallel, light stress-recovery experiments (LSRE) were carried out in controlled conditions in the laboratory at two temperatures using freshly collected samples (see section below). During LSRE, samples were sequentially exposed to (i) low light (LL) level to determine pre-stress reference state; (ii) high light (HL) intensity to induce photoinhibitory effects; (iii) LL to monitor recovery from HL stress (Serôdio *et al.*, 2012).

In situ *measurements*

For each site, the day for carrying out the experiment was selected so that the emersion period matched with maximum light and temperature exposure, i.e. noon/early afternoon low tides. Photosynthetic Active Radiation (PAR) and temperature at the surface of the sediment were assessed every 30 s with a universal light-meter and data logger (ULM-500, Walz Effeltrich Germany) equipped with a plane light/temperature sensor (accessory of the ULM-500) and a plane cosine quantum sensor (Li-COR). Depth temperature profiles were measured with Hobo sensors (Hobo Pro V2, Massachussets, USA) fixed on a home-made stick that was vertically inserted into the sediment to position the sensors at four (-0.5 cm, -2 cm, -5 cm, -10 cm). The

effective photosystem II quantum yield (ΦPSII) and the non-photochemical quenching of chlorophyll *a* (Chl *a*) fluorescence (NPQ) of MPB was assessed with a Water-PAM (micro-fiber version, Walz GmbH, Effeltrich, Germany) as described in Lefebvre *et al.* (2011). ΦPSII was calculated as $\Delta F / F_m' = (F_m - F) / F_m'$. Rapid light curves (RLCs) with 30 s light steps were used to measure NPQ *vs* irradiance (NPQ-E) curves (as recommended in Lefebvre *et al.*, 2011). NPQ-E curves were fitted with the model by Serôdio and Lavaud (2011) in order to estimate NPQ_{max} where $NPQ = (F_m - F_m') / F_m$. F_m and F_m' are the maximum Chl *a* fluorescence levels measured in dark-adapted and illuminated (at the end of each RLCs light steps) MPB, respectively, while F is the steady-state Chl *a* fluorescence level measured at the end of each RLC light step, just before F_m' was assessed. F was measured with the application of a non-actinic modulated beam of 455 nm, and F_m and F_m' with the application of over-saturating (about 4000 µmol photons m^{-2} s^{-1}) light pulses (800 ms). Because in *in situ* as well as in laboratory (see below) conditions (i.e. light-responsive migratory biofilm) it is virtually impossible to measure a true F_m level, for the calculation of NPQ, F_m was in reality the maximum F_m' of the respective RLC (i.e. $F_m'_{max} \sim F_m$, see Lefebvre *et al.*, 2011).

Light stress-recovery experiments (LSRE)

LSRE were carried out following a protocol adapted from Serôdio *et al.* (2012). The top 1 cm of sediment was collected at the beginning of low tide and immediately transported to the laboratory where it was sieved (0.5 mm mesh) to remove debris and macrofauna. Sediment was thoroughly mixed and spread in trays, forming a 2-4 cm thick slurry, and it was covered with seawater from the sampling site and left undisturbed overnight in the dark at room temperature (~20-25°C). The next morning, the slurry was homogenized and transferred to 24-well plates using a 100 mL syringe, filling the wells completely (ca. 3 mL). The well plates were then exposed to constant LL of 50 µmol photons m^{-2} s^{-1}, provided by three slide

projectors (Reflecta Diamator AF, Reflecta GmbH, Rottenburg, Germany) containing halogen lamps (Quartzline DDL 150W, General Electric, USA) to induce the upward migration of MPB. Once the MPB biofilm was formed (typically after 3 h), the plates were transferred to a water bath of constant temperature of 25°C or 40°C and exposed to constant LL for 30 min. These two experimental temperatures were defined based on a previous study (Blanchard *et al.*, 1997) which defined 25°C as an optimum and 35-40°C as an extreme maximum for the photosynthetic productivity of MPB. A fixed volume (200 µL) of Lat A solution (10 µM final concentration) or of filtered sea water (Control samples: Ctrl) was added to each well. Lat A solution was freshly prepared daily from a 1 mM stock solution of purified Lat A (Sigma-Aldrich) dissolved in dimethylsulfoxide and stored at -20°C (Cartaxana and Serôdio, 2008). After 15 min waiting for the inhibitor to diffuse, the plates were exposed to HL (1200 µmol photons m^{-2} s^{-1}, 3 h). This light dose (12.96 mol photons m^{-2}) was previously shown to be excessive for MPB photosynthesis (Serôdio *et al.*, 2012). After 3 h, samples were placed under LL for 15 min. In parallel, additional samples (for both Ctrl and +Lat A treatments) were maintained during 3 h under continuous LL. Temperature of the sediment in the top 5 mm was regularly checked using the same sensor previously described. The duration of each step described above was always the same, but the timing was adjusted so that HL period always started at the low tide maximum expected *in situ*.

For each chemical and light treatment (Ctrl and +Lat A; HL or continuous LL), several endpoints were assessed on 3-6 independent samples at three times: just before the HL stress (T_0), at the end of the HL stress and after 15 min of LL recovery (Recov). For the experiments with FR samples, Chl *a* fluorescence was measured using an Imaging-PAM fluorometer (Maxi-PAM M-series, Walz GmbH, Effeltrich, Germany) and samples were collected for further quantification of photosynthetic pigments, lipid peroxidation, and Lhcx proteins. For PT samples, Chl *a* fluorescence was measured with a FluorCAM 800MF, open version (PSI,

530 Brno, Czech Republic, see Serôdio *et al.*, 2013). Samples were collected for the same
531 analyses than for FR site, except that pigments were not quantified. Samples were collected
532 for the same analyses than for FR site, except that pigments were not quantified. ΦPSII and
533 NPQ were calculated as previously described (Serôdio *et al.*, 2012).
534 For the sediment sampling in wells, a contact-corer specially designed was used to collect
535 rapidly (< 30 s) the uppermost layer of sediment (0.5 mm thick, 1.5 cm^2 area) in each well. It
536 is based on the cryo-sampling of the biofilm, through the contact of the sediment surface with
537 a metal cylinder of known length previously cooled in liquid nitrogen (Laviale *et al.*,
538 submitted). Each core was immediately frozen in liquid nitrogen and stored at -80°C until
539 further analysis.
540
541 *Pigment analysis*
542 Pigment extraction and HPLC analysis were carried out following Lepetit *et al.* (2013), with
543 the exception of the first extraction step which was performed after 24 h lyophilisation of the
544 sediment cores (3 mL of 4°C mixture extraction buffer: 90% methanol/0.2 M ammonium
545 acetate (90/10 vol/vol) + 10% ethyl acetate). Extracted samples were analyzed with a Hitachi
546 LaChrom Elite HPLC system equipped with a 10°C-cooled autosampler and a Nucleosil 120-
547 5 C18 column (Macherey-Nagel). The allomerization of Chl *a* was calculated as the ratio AR
548 = Chl *a*-allo / tot Chl *a* × 100 where tot Chl *a* = (Chl *a*-allo + Chl *a*' + Chl *a*) and Chl *a*-allo
549 and Chl *a*' are the allomer and epimer forms of Chl *a*, respectively. The pigment molar
550 concentrations (expressed as mol. 100 mol Chl a^{-1}) for the xanthophyll cycle (XC) pigments
551 diadinoxanthin (DD) and diatoxanthin (DT) were used to calculate the DD de-epoxidation
552 state (DES) as follows: DES = [DT / (DD + DT)] × 100.
553
554 *Lipid peroxidation*

555 Lipid peroxidation generated by oxidative stress was estimated by quantifying thiobarbituric
556 acide reactive substances (TBARS) according to Kwon and Watts (1964). Each sample was
557 resuspended in 0.8 mL of 10% trichloroacetic acid (TCA, Sigma-Aldrich) and 500 mg L^{-1}
558 butylated hydroxytoluene (BHT, Sigma-Aldrich) and sonicated (U200S control; IKA
559 Labortechnik, Ika-Werke GmbH, Staufen, Germany) on ice 5 times during 30 s (cycle: 1,
560 amplitude: 30%) with intervals of 30 s to prevent overheating. After extraction, 0.8 mL of
561 0.5% thiobarbituric acid (TBA, Sigma-Aldrich) in 10% TCA was added. The mixture was
562 heated for 30 min at 90 °C and immediately put on ice to stop the reaction. Samples were then
563 centrifuged (15 min, 10000 g) and 250 µL of supernatant were transferred in a 96 well-plate
564 (Sarsted). TBARS were measured by subtracting the nonspecific turbidity (at 600 nm) from
565 the TBARS absorption maximum (532 nm) using a Synergy HT absorbance microplate reader
566 (BioTek Instruments Inc., Vermont, USA). Blanks consisted of the same mixture without
567 sediment sample. TBARS concentration was expressed in malondialdehyde (MDA)
568 equivalent (nmol mL^{-1}) using an extinction coefficient of 155 mM^{-1} cm^{-1}. As it was not
569 possible to obtain paired measurements of Chl *a* and MDA, values were normalized to the
570 microphytobenthos biomass present at the sediment surface (measured by spectral reflectance:
571 see below). As migration was susceptible to occur in Ctrl samples, only Lat A-treated samples
572 could be compared.
573
574 *MPB surface biomass*
575 MPB biomass present in the surface layers of the sediment was estimated by spectral
576 reflectance analysis with a fiber optic spectrometer (USB2000-VIS-NIR, grating #3, Ocean
577 Optics, Duiven, The Netherlands) according to Serôdio *et al.* (2009). In particular,
578 measurements were carried out under LL (50 µmol photons m^{-2} s^{-1}) supplied with an halogen
579 lamp (120W, Plusline ES, Philips Lighting) positioned with a 45° angle to the sediment

surface while the sensor was at a fixed distance (~2 cm) perpendicularly to it. Reflectance measurements at 550, 600 and 675 nm (ρ_{550}, ρ_{600} and ρ_{675}, respectively) were used to calculate the normalized index I_{diat} as follows: $I_{diat} = 2 \times \rho_{600} / (\rho_{550} + \rho_{675})$ (modified from Kazemipour et al 2012). It is based on the spectral peak centered at 600 nm between the absorbance bands due to the fucoxanthin at 550 nm and the Chl *a* at 675 nm. In comparison to other MPB spectral indices available (Méléder *et al.*, 2010), it was shown to be less affected by water or detritical organic matter contents, thus allowing a better comparison between sites (data not shown).

Lhcx protein analysis

Protein extraction from sediment cores, SDS-PAGE, Western-blot and ECL immunodetection were carried out following the protocol by Coesel et al. (2009) modified by Lepetit *et al.* (2013): In order to improve the proteins extraction, sediment samples were exposed to eight freeze thaw cycles in the extraction buffer (500 µL lysis buffer + 500 µL protease inhibitor, Sigma-Aldrich, USA) and then incubated at RT (total extraction was 90 min). Chl *a* concentration of extracted samples was determined according to Jeffrey and Humphrey (1975) and samples corresponding to an amount of 0.5 µg Chl *a* were loaded on the gel. Correct blotting was verified by correct transfer of pre-stained protein markers on the PVDF membrane (Amersham Hybond-P, GE Healthcare life Sciences, USA) and by staining gels with Coomassie R-250 (Pierce Imperial Protein stain, Thermo scientific, Rockford, USA). Anti-FCP6 (Lhcx1) from *Cyclotella cryptica* (Westermann and Rhiel, 2005) and anti-Lhcx6 from *T. pseudonana* (Zhu and Green, 2010) were applied in a 1:1000 dilution for LR samples overnight (respective incubations with the secondary antibody were 2 h and 1 h). For PT samples, the anti-Lhcx6 antibody did not yield a good signal; anti-FCP6 was used at a dilution of 1:1000 (incubation with the secondary antibody, 1 h). Note that because of the species-

specific immunodetection pattern no quantification *per se* was possible. However, the comparison with the planktonic models *P. tricornutum* (Bailleul *et al.*, 2010; Lepetit *et al.*, 2013) and *T. pseudonana* (Zhu *et al.*, 2010) enabled to possibly distinguish different isoforms including some for which behaviour under HL and temperature stress and their role is known or suspected (see Introduction; Bailleul *et al.*, 2010; Zhu *et al.*, 2010; Lepetit *et al.*, 2013; Büchel, 2014). For *P. tricornutum*, *T. pseudonana* and *N. phyllepta* samples, the procedure was as in Lepetit *et al.* (2013): exponentially growing cells were exposed to HL stress (2 h at 2000 µmol photons. m^{-2}. s^{-1}) to induce protein expression of several Lhcx isoforms which were separated on the LDS-gel.

Taxonomic composition

For each site, the first cm of sediment was collected and stored at -20 °C until analysis. Extraction from sediment of the organic fraction, including microalgae cells, was done following Méléder *et al.* (2007). Preliminary observations of the organic fraction using optical microscopy (Olympus AX70 using 200-fold magnification) were performed to confirm the absence of other classes of microalgae than diatoms. Permanent slides of cleaned diatom frustules (cremation: 2 h at 450 °C) were then prepared in a high refractive index medium (Naphrax; Northern Biological Supplies Ltd, Ipswich, UK). The taxonomic composition was determined to the species level by examining 200-300 frustule valves at 500 fold magnification on the basis of morphological criteria using reference works (Ribeiro *et al.*, 2013, and references therein). Scanning electron microscopy was used to confirm the analysis (JEOL JSM 7600F reaching 50 000-fold magnification).

Statistics

629 Data presented are mean ± one standard deviation (SD). Each LSRE experiment was
630 performed twice. Analyses of variance (ANOVA), Tukey's honestly significant difference
631 (HSD) tests, Student's t-tests and linear regressions were performed using the R statistical
632 computing environment (v 2.15.1, Ihaka and Gentleman, 1996). In particular, potential
633 interactions between factors were tested considering data set from each site individually, with
634 time (T_0, after 3 h of HL, after 15 min recovery under LL), temperature (27°C and 37°C) and
635 chemical (Ctrl or +Lat A) as fixed factors. The fact that Chl *a* fluorescence measurements
636 were made on the same samples over the experiment was also taken into account using the
637 sample name as random effect in a linear mixed effect model (lme function of the nlme
638 package: Pinheiro and Bates, 2000). Comparisons between sites (FR, PT) were performed on
639 data gathered at the end of the LSRE (after recovery), expressed as % of T_0. Site, temperature
640 and chemical were considered as fixed factors. Data normality (Shapiro-Wilk test) and
641 homoscedasticity (Bartlett test) were checked using the residuals.
642

643 **Acknowledgements**

644 The present study was supported by the Egide/Campus France-PHC Pessoa exchange
645 program (n°27377TB, JL and JS), the Centre National de la Recherche Scientifique-CNRS
646 (JL), the University of La Rochelle-ULR and the Contrat Plan Etat Région-CPER 'Littoral'
647 (JL, BL post-doc grant), the Region Poitou-Charentes (AB Ph.D. grant), the Deutscher
648 Akademischer Austausch Dienst-DAAD (BL post-doc grant), European Funds through
649 COMPETE, the Portuguese Science Foundation (FCT) through projects PEST (PEst-
650 C/MAR/LA0017/2013) and MigROS (PTDC/MAR/112473/2009: JS, ML post-doc grant and
651 SF research assistant grant), and through grants SFRH/BSAB/962/2009 (JS), SFRH/BD/
652 44860/2008 (JE Ph.D. grant). The authors thank Dr. E. Rhiel (Univ. Oldenburg, Germany)
653 and Prof. B. Green (Univ. British Columbia, Canada) for the kind gifts of the anti-FCP6 and
654 of the anti-Lhcx6, respectively, Prof. B. Green for her help analyzing the Lhcx6 Western-blot,
655 C. Pais for her technical assistance with the TBARS quantification, Dr L. Ribeiro (Univ.
656 Lisboa, Portugal) for his help in confirming the identification of *N. phyllepta* s.l., and Sr
657 Armindo do Evaristo for his cheerful support. We thank the two anonymous reviewers for
658 their constructive comments on the manuscript.

659

660 **References**

661 Admiraal, W. (1984) The ecology of estuarine sediment inhabiting diatoms. *Prog Phycol Res*
662 **3**: 269-322.

663 Bailleul, B., Rogato, A., de Martino, A., Coesel, S., Cardol, P., Bowler, C. et al. (2010) An
664 atypical member of the light-harvesting complex stress-related protein family modulates
665 diatom responses to light. *Proc Natl Acad Sci USA* **107**: 18214-18219.

666 Barnett, A., Méléder, M., Blommaert, L., Lepetit, B., Gaudin, P., Vyverman, W. et al. (2014)
667 Growth form defines physiological photoprotective capacity in intertidal benthic diatoms.
668 *ISME J* doi:10.1038/ismej.2014.105.

669 Blanchard, G.F., Guarini, J.M., Gros, P., and Richard, P. (1997) Seasonal effect on the
670 relationship between the photosynthetic capacity of intertidal microphytobenthos and
671 temperature. *J Phycol* **33**: 723-728.

672 Blanchard, G.F., Guarini, J.M., Richard, P., Gros, P., and Mornet, F. (1996) Quantifying the
673 short-term temperature effect on light-saturated photosynthesis of intertidal
674 microphytobenthos. *Mar Ecol Prog Ser* **134**: 309-313.

675 Brito, A.C., Benyoucef, I., Jesus, B., Brotas, V., Gernez, P., Mendes, C.R. et al. (2013)
676 Seasonality of microphytobenthos revealed by remote-sensing in a South European
677 estuary. *Cont Shelf Res* **66**: 83-91.

678 Brunet, C., and Lavaud, J. (2010) Can the xanthophyll cycle help extract the essence of the
679 microalgal functional response to a variable light environment? J *Plankton Res* **32**: 1609-
680 1617.

681 Büchel, C. (2014) Fucoxanthin-chlorophyll-proteins and non-photochemical fluorescence
682 quenching in diatoms. In *Non-Photochemical Fluorescence Quenching and Energy*
683 *Dissipation In Plants, Algae and Cyanobacteria*. Demmig-Adams, B., Garab, G., Adams,
684 W.W.III, and Govindjee (eds). Advances in Photosynthesis and Respiration, Volume 40.,

685 pp 259-275. Dordretch, The Netherlands: Springer.
686 Cartaxana, P., and Serôdio, J. (2008) Inhibiting diatom motility: a new tool for the study of
687 the photophysiology of intertidal microphytobenthic biofilms. *Limnol Oceanogr-Meth*. **6**:
688 466-476.
689 Cartaxana, P., Ruivo, M., Hubas, C., Davidson, I., Serôdio, J., and Jesus, B. (2011)
690 Physiological versus behavioral photoprotection in intertidal epipelic and epipsammic
691 benthic diatom communities. *J Exp Mar Biol Ecol* **405**: 120-127.
692 Cartaxana, P., Domingues, N., Cruz, S., Jesus, B., Laviale, M., Serôdio, J., and da Silva, J.M.
693 (2013) Photoinhibition in benthic diatom assemblages under light stress. *Aquat Microb*
694 *Ecol* **70**: 87-92.
695 Chevalier, E.M., Gévaert, F., and Créach, A. (2010) In situ photosynthetic activity and
696 xanthophylls cycle development of undisturbed microphytobenthos in an intertidal
697 mudflat. *J Exp Mar Biol Ecol* **385**: 44-49.
698 Cid, A., Herrero, C., Torres, E., and Abalde, J. (1995) Copper toxicity on the marine
699 microalga *Phaeodactylum tricornutum* - Effects on photosynthesis and related parameters.
700 *Aquat Toxicol* **31**: 165-174.
701 Coelho, H., Vieira, S., and Serôdio, J. (2011) Endogenous versus environmental control of
702 vertical migration by intertidal benthic microalgae. *Eur J Phycol* **46**: 271-281.
703 Coesel, S., Mangogna, M., Ishikawa, T., Heijde, M., Rogato, A., Finazzi, G., Todo, T.,
704 Bowler, C., Falciatore, A. (2009) Diatom PtCPF1 is a new cryptochrome/photolyase
705 family member with DNA repair and transcription regulation activity. *EMBO Rep* **10**:
706 655–661.
707 Cohn, S.A., Farrell, J.F., Munro, J.D., Ragland, R.L., Weitzell, R.E., and Wibisono, B.L.
708 (2003) The effect of temperature and mixed species composition on diatom motility and
709 adhesion. *Diatom Res* **18**: 225-243.

710 Consalvey, M., Paterson, D.M., and Underwood, G.J.C. (2004) The ups and downs of life in a
711 benthic biofilm: Migration of benthic diatoms. *Diatom Res* **19**: 181-202.
712 Davison, I.R. (1991) Environmental effects on algal photosynthesis - Temperature. *J Phycol*
713 **27**: 2-8.
714 Depauw, F.A., Rogato, A., d'Alcala, M.R., and Falciatore, A. (2012) Exploring the molecular
715 basis of responses to light in marine diatoms. *J Exp Bot* **63**: 1575-1591.
716 Du, G.Y., J.H., O., Li, H., and Chung, I.K. (2010) Effect of light and sediment grain size on
717 the vertical migration of benthic diatoms. *Algae* **25**: 133-140.
718 Du, G.Y., Li, W.T., Li, H.B., and Chung, I.K. (2012) Migratory responses of benthic diatoms
719 to light and temperature monitored by chlorophyll fluorescence. *J Plant Biol* **55**: 159-164.
720 Goss, R., and Jakob, T. (2010) Regulation and function of xanthophyll cycle-dependent
721 photoprotection in algae. *Photosynth Res* **106**: 103-122.
722 Goss, R., Pinto, E.A., Wilhelm, C., and Richter, M. (2006) The importance of a highly active
723 and delta pH-regulated diatoxanthin epoxidase for the regulation of the PSII antenna
724 function in diadinoxanthin cycle containing algae. *J Plant Physiol* **163**: 1008-1021.
725 Grant, J. (1986) Sensitivity of benthic community respiration and primary production to
726 changes in temperature and light. *Mar Biol* **90**: 299-306.
727 Guarini, J.M., Blanchard, G.F., and Richard, P. (2006) Modelling the dynamic of the
728 microphytobenthic biomass and primary production in European intertidal mudflats. In
729 *Functioning of microphytobenthos in estuaries*. Kromkamp, J.C., de Brouwer, J.F.C.,
730 Blanchard, G.F., Forster, R.M., and Créach, V. (eds). Amsterdam, the Netherlands:
731 KNAW, pp. 187-226.
732 Guarini, J.M., Blanchard, G.F., Gros, P., and Harrison, S.J. (1997) Modelling the mud surface
733 temperature on intertidal flats to investigate the spatio-temporal dynamics of the benthic
734 microalgal photosynthetic capacity. *Mar Ecol Prog Ser* **153**: 25-36.

735 Hancke, K., and Glud, R.N. (2004) Temperature effects on respiration and photosynthesis in
736 three diatom-dominated benthic communities. *Aquat Microb Ecol* **37**: 265-281.
737 Hancke, K., Sorell, B.K., Chresten, L., Lund-Hansen, L.C., Larsen, M., Hancke, T., and Glud,
738 R.N. (2014) Effects of temperature and irradiance on a benthic microalgal community: A
739 combined two-dimensional oxygen and fluorescence imaging approach. *Limnol.*
740 *Oceanogr*. **59**: 1599–1611.
741 Haubois, A.G., Sylvestre, F., Guarini, J.M., Richard, P., and Blanchard, G.F. (2005) Spatio-
742 temporal structure of the epipelic diatom assemblage from an intertidal mudflat in
743 Marennes-Oleron Bay, France. *Estuar Coast Shelf S* **64**: 385-394.
744 Hicks, N. Bulling, M.T., Solan, M., Raffaelli, D., White, P.C.L., and Paterson, D.M. (2011)
745 Impact of biodiversity-climate futures on primary production and metabolism in a model
746 benthic estuarine system. *BMC Ecology*. **11**: 7.
747 Hynninen, P.H., Kaartinen, V., and Kolehmainen, E. (2010) Horseradish peroxidase-catalyzed
748 oxidation of chlorophyll a with hydrogen peroxide Characterization of the products and
749 mechanism of the reaction. *BBA-Bioenergetics* **1797**: 531-542.
750 Hwang, Y.-S., Jung, G., and Jin, E. (2008) Transcriptome analysis of acclimatory responses to
751 thermal stress in Antarctic algae. *Biochem Bioph Res Co* **367**: 635-641
752 Ihaka, R., and Gentleman, R. (1996) R: a language for data analysis and graphics. *J Comput*
753 *Graph Stat* **5**: 299-314.
754 Jeffrey, S.W., and Humphrey, G.F. (1975) New spectrophotometric equations for determining
755 chlorophylls a, b c1 and c2 in higher-plants, algae and natural phytoplankton. *Biochem*
756 *Physiol Pfl* **167**: 191-194.
757 Jesus, B., Brotas, V., Ribeiro, L., Mendes, C.R., Cartaxana, P., and Paterson, D.M. (2009)
758 Adaptations of microphytobenthos assemblages to sediment type and tidal position. *Cont*
759 *Shelf Res* **29**: 1624-1634.

760 Kazemipour, F., Launeau, P., and Meleder, V. (2012) Microphytobenthos biomass mapping
761 using the optical model of diatom biofilms: Application to hyperspectral images of
762 Bourgneuf Bay. *Remote Sens Environ* **127**: 1-13.
763 Kromkamp, J., Barranguet, C., and Peene, J. (1998) Determination of microphytobenthos PSII
764 quantum efficiency and photosynthetic activity by means of variable chlorophyll
765 fluorescence. *Mar Ecol Prog Ser* **162**: 45-55.
766 Kwon, T., and Watts, B.M. (1964) Malonaldehyde in aqueous solution and its role as measure
767 of lipid oxidation in foods. *J Food Sci* **29**: 294-302.
768 Lavaud, J., and Lepetit, B. (2013) An explanation for the inter-species variability of the
769 photoprotective non-photochemical chlorophyll fluorescence quenching in diatoms. *BBA-*
770 *Bioenergetics* **1827**: 294-302.
771 Lavaud, J., and Goss, R. (2014) The peculiar features of non-photochemical fluorescence
772 quenching in diatoms and macrophytic brown algae. In *Non-Photochemical Fluorescence*
773 *Quenching and Energy Dissipation In Plants, Algae and Cyanobacteria*. Demmig-Adams,
774 B., Garab, G., Adams, W.W.III, and Govindjee (eds). Advances in Photosynthesis and
775 Respiration, Volume 40, pp 421-443. Dordretch, The Netherlands: Springer.
776 Lavaud, J., Materna, A.C., Sturm, S., Vugrinec, S., and Kroth, P.G. (2012) Silencing of the
777 violaxanthin de-epoxidase gene in the diatom *Phaeodactylum tricornutum* reduces
778 diatoxanthin synthesis and non-photochemical quenching. *Plos One* **7**: e36806.
779 Laviale, M., Ezequiel, J., Pais, C., Cartaxana P. and Serôdio, J. (submitted) A new high-
780 resolution method for the fast vertical sampling of intertidal fine sediments.
781 Lefebvre, S., Mouget, J.L., and Lavaud, J. (2011) Duration of rapid light curves for
782 determining the photosynthetic activity of microphytobenthos biofilm in situ. *Aquat Bot*
783 **95**: 1-8.
784 Lepetit, B., Volke, D., Gilbert, M., Wilhelm, C., and Goss, R. (2010) Evidence for the

785 existence of one antenna-associated, lipid-dissolved and two protein-bound pools of
786 diadinoxanthin cycle pigments in diatoms. *Plant Physiol* **154**: 1905-1920.
787 Lepetit, B., Goss, R., Jakob, T., and Wilhelm, C. (2012) Molecular dynamics of the diatom
788 thylakoid membrane under different light conditions. *Photosynth Res* **111**: 245-257.
789 Lepetit, B., Sturm, S., Rogato, A., Gruber, A., Sachse, M., Falciatore, A., Kroth, P.G., and
790 Lavaud, J. (2013) High light Acclimation in the secondary plastids containing diatom
791 *Phaeodactylum tricornutum* is triggered by the redox state of the plastoquinone pool.
792 *Plant Physiol* **161**: 853-865.
793 Lillebo, A.I., Valega, M., Otero, M., Pardal, M.A., Pereira, E., and Duarte, A.C. (2010) Daily
794 and inter-tidal variations of Fe, Mn and Hg in the water column of a contaminated salt
795 marsh: Halophytes effect. *Estuar Coast Shelf S* **88**: 91-98.
796 Mathur, S., Agrawal, D., and Jajoo, A. (2014) Photosynthesis: Response to high temperature
797 stress. *J Photoch Photobio B* **137**: 116-126
798 Méléder, V., Rincé, Y., Barillé, L., Gaudin, P., and Rosa, P. (2007) Spatiotemporal changes in
799 microphytobenthos assemblages in a macrotidal flat (Bourgneuf bay, France). *J Phycol*
800 **43**: 1177-1190.
801 Méléder, V., Launeau, P., Barillé, L., Combe, J.-P. , Carrère V., Jesus, B., and Verpoorter, C.
802 (2010) Hyperspectral imaging for mapping microphytobenthos in coastal areas. In:
803 *Geomatic solutions for coastal environments*. Maanan, M., and Robin, M. (eds). Nova
804 Science Publishers.

805 Morris, E.P., and Kromkamp, J.C. (2003) Influence of temperature on the relationship
806 between oxygen- and fluorescence-based estimates of photosynthetic parameters in a
807 marine benthic diatom (*Cylindrotheca closterium*). *Eur J Phycol* **38**: 133-142.
808 Paterson, D.M., and Hagerthey, S.E. (2001) Microphytobenthos in contrasting coastal
809 ecosystems: Biology and dynamics. In *Ecological Comparison of Sedimentary Shores*.

Reise, K. (ed). Berlin Heildelberg: Springer-Verlag, pp. 105-125.

Perkins, R.G., Lavaud, J., Serôdio, J., Mouget, J.L., Cartaxana, P., Rosa, P. et al. (2010) Vertical cell movement is a primary response of intertidal benthic biofilms to increasing light dose. *Mar Ecol Prog Ser* **416**: 93-103.

Pinheiro, J.C., and Bates, D.M. (2000) *Mixed-models in S and S-PLUS*. New York, USA: Springer-Verlag.

Ribeiro, L., Brotas, V., Rince, Y., and Jesus, B. (2013) Structure and diversity of intertidal benthic diatom assemblages in contrasting shores: A case study from the Tagus estuary. *J Phycol* **49**: 258-270.

Rijstenbil, J.W. (2005) UV- and salinity-induced oxidative effects in the marine diatom *Cylindrotheca closterium* during simulated emersion. *Mar Biol* **147**: 1063-1073.

Roncarati, F., Rijstenbil, J.W., and Pistocchi, R. (2008) Photosynthetic performance, oxidative damage and antioxidants in *Cylindrotheca closterium* in response to high irradiance, UVB radiation and salinity. *Mar Biol* **153**: 965-973.

Saburova, M.A., and Polikarpov, I.G. (2003) Diatom activity within soft sediments: behavioural and physiological processes. *Mar Ecol Prog Ser* **251**: 115-126.

Salleh, S., and McMinn, A. (2011) The effects of temperature on the photosynthetic parameters and recovery of two temperate benthic microalgae, *Amphora cf. coffeaeformis* and *Cocconeis* cf. *sublittoralis* (Bacillariophyceae). *J Phycol* **47**: 1413-1424.

Schär, C., Vidale P.L., Lüthi, D., Frei, C., Häberli, C., Liniger, M.A., and Appenzeller, C. (2004) The role of increasing temperature variability in European summer heatwaves. *Nature* **427**: 332-336.

Serôdio, J., and Catarino, F. (1999) Fortnightly light and temperature variability in estuarine intertidal sediments and implications for microphytobenthos primary productivity. *Aquat. Ecol.* **33**: 235-241.

835 Serôdio, J., Cartaxana, P., Coelho, H., and Vieira, S. (2009) Effects of chlorophyll
836 fluorescence on the estimation of microphytobenthos biomass using spectral reflectance
837 indices. *Remote Sens Environ* **113**: 1760-1768.
838 Serôdio, J., and Lavaud, J. (2011) A model for describing the light response of the
839 nonphotochemical quenching of chlorophyll fluorescence. *Photosynth Res* **108**: 61-76.
840 Serôdio, J., Cruz, S., Vieira, S., and Brotas, V. (2005) Non-photochemical quenching of
841 chlorophyll fluorescence and operation of the xanthophyll cycle in estuarine
842 microphytobenthos. *J Exp Mar Biol Ecol* **326**: 157-169.
843 Serôdio, J., Ezequiel, J., Frömmlet, J., Laviale, M., and Lavaud, J. (2013) A method for the
844 rapid generation of non-sequential light-response curves of chlorophyll fluorescence.
845 *Plant Physiol* **163**: 1089-1102.
846 Serôdio, J., Ezequiel, J., Barnett, A., Mouget, J.L., Méléder, V., Laviale, M., and Lavaud, J.
847 (2012) Efficiency of photoprotection in microphytobenthos: role of vertical migration and
848 the xanthophyll cycle against photoinhibition. *Aquat Microb Ecol* **67**: 161-175.
849 Solomon, S., Qin, D., Manning, M., Chen, Z., Marquis, M., Averyt, K.B., Tignor, M., and
850 Miller, H.L. (eds.) (2007) Contribution of Working Group I to the Fourth Assessment
851 Report of the Intergovernmental Panel on Climate Change. In *Climate Change 2007:*
852 *Impacts, Adaptation and Vulnerability.* 996 pp., Cambridge University Press, Cambridge,
853 United Kingdom and New York, NY, USA.
854 Stott, P.A., Stone, D.A., and Allen, M.R. (2004) Human contribution to the European
855 heatwave of 2003. *Nature* **432**: 610-614.
856 Underwood, G.J.C., and Kromkamp, J. (1999) Primary production by phytoplankton and
857 microphytobenthos in estuaries. In *Advances in Ecological Research, Vol 29: Estuaries*,
858 pp. 93-153.
859 van Leeuwe, M.A., Brotas, V., Consalvey, M., Forster, R.M., Gillespie, D., Jesus, B. et al.

(2008) Photoacclimation in microphytobenthos and the role of xanthophyll pigments. *Eur J Phycol* **43**: 123-132.

Vanelslander, B., Creach, V., Vanormelingen, P., Ernst, A., Chepurnov, V.A., Sahan, E. et al. (2009) Ecological differentation between sympatric pseudocryptic species in the estuarine benthic diatom *Navicula phyllepta* (Bacillariophyceae). *J Phycol* **45**: 1278-1289.

Vieira, S., Ribeiro, L., da Silva, J.M., and Cartaxana, P. (2013) Effects of short-term changes in sediment temperature on the photosynthesis of two intertidal microphytobenthos communities. *Estuar Coast Shelf S* **119**: 112-118.

Wang, Z.-H., Nie, X.-P., Yue, W.-J., and Li, X. (2012) Physiological responses of three marine microalgae exposed to cypermethrin. *Environ Toxicol* **27**: 563-572.

Waring, J., Klenell, M., Bechtold, U., Underwood, G.J.C., and Baker, N.R. (2010) Light-induced responses of oxygen photoreduction, reactive oxygen species production and scavenging in two diatom species. *J Phycol* **46**: 1206-1217.

Westermann, M., and Rhiel, E. (2005) Localisation of fucoxanthin chlorophyll a/c-binding polypeptides of the centric diatom *Cyclotella cryptica* by immuno-electron microscopy. *Protoplasma* **225**: 217-223.

Witkowski, A., Sullivan, M.J., Bogaczewicz-Adamczak, B., Bak, M., Rhiel, E., Ribeiro, L., and Richard, P. (2012) Morphology and distribution of a little known but widespread diatom (Bacillariophyceae), *Navicula spartinetensis* Sullivan et Reimer. *Diatom Res* **27**: 43-51.

Wu, H.Y., Roy, S., Alami, M., Green, B.R., and Campbell, D.A. (2012) Photosystem II photoinactivation, repair, and protection in marine centric diatoms. *Plant Physiol* **160**: 464-476.

Yun, M.S., Lee, S.H., and Chung, I.K. (2010) Photosynthetic activity of benthic diatoms in response to different temperatures. *J Appl Phycol* **22**: 559-562.

885 Zhu, S.H., and Green, B.R. (2010) Photoprotection in the diatom *Thalassiosira pseudonana*:
886 Role of LI818-like proteins in response to high light stress. *BBA-Bioenergetics* **1797**:
887 1449-1457.
888

889 **Figure legends**

890 **Figure 1**

891 **In situ environmental conditions and photosynthetic activity of microphytobenthos**
892 **during a summer diurnal emersion in Portuguese (Ria de Aveiro, Vista Alegre, A- and**
893 **C-) and French (Baie de l'Aiguillon, Esnandes, B- and D-) intertidal flats.** A- and B-
894 Photosynthetic Active Radiation (PAR, µmol photons m^{-2} s^{-1}, black line) at the surface of the
895 sediment and temperature (°C) at five depths (surface, -0.5 cm, -2 cm, -5 cm, -10 cm, grey
896 lines); C- and D- effective PSII quantum yield (ΦPSII: open squares) and maximum non-
897 photochemical quenching of Chl *a* fluorescence (NPQ_{max}: closed circles). Local time (FR:
898 UTC+1, PT: UTC).

899

900 **Figure 2**

901 **Index of photoinhibition (decrease in ΦPSII) of microphytobenthos harvested at the**
902 **French site (FR) during light stress recovery experiments performed on sediment**
903 **exposed at two temperatures (27°C, A- or 37°C, B-) and with an inhibitor of cell motility**
904 **(+ Lat A) or without (Ctrl).** T_0, beginning of the experiment under low light (50 µmol
905 photons m^{-2} s^{-1}); HL, after 3 h high light (1200 µmol photons m^{-2} s^{-1}); Recov, after 15 min
906 recovery under low light (50 µmol photons m^{-2} s^{-1}) following the 3 h high light; LL, after 3 h
907 of low light (50 µmol photons m^{-2} s^{-1}). Values are mean ± SD (n=6).

908

909 **Figure 3**

Index of photoprotection (NPQ) of microphytobenthos harvested at the French site (FR) during light stress recovery experiments performed on sediment exposed at two temperatures (27°C, A- or 37°C, B-) and with an inhibitor of cell motility (+Lat A) or without (Ctrl). Legend as in Fig. 2**.** Values are mean ± SD (n=6).

Figure 4

Pigment content makers of photooxidative stress (Chl *a* allomerization ratio: AR) and of photoprotection (DD+DT pool; DD de-epoxidation state: DES) of microphytobenthos harvested at the French site (FR) during light stress recovery experiments performed on sediment exposed at two temperatures (27°C or 37°C) and with an inhibitor of cell motility (+Lat A) or without (Ctrl). A- AR, data from 27 and 37°C experiments were pooled, * significant difference compared to Ctrl at the same time ($P < 0.05$, Tukey HSD); B- DD+DT pool (in mol.100 mol Chl a^{-1}), data from Ctrl and Lat A-treated samples were pooled, ** significant difference compared to 27 °C at the same time ($P < 0.01$, Tukey HSD); C- and D- DES, *** significant difference compared to Ctrl at the same time ($P < 0.001$, Tukey HSD). Labels as in Fig. 2. Values are mean ± SD (n=12: A,B or n=6: C,D) expressed as $\%T_0$.

Figure 5

Western blot of the Lhcx proteins of microphytobenthos harvested at the French site during light stress recovery experiments performed on sediment exposed at two temperatures (27°C, A- or 37°C, B-) and with an inhibitor of cell motility (+) or without (-). HL, after 3 h HL (1200 µmol photons m^{-2} s^{-1}); LL, after 3 h of LL (50 µmol photons m^{-2} s^{-1}). All samples were normalized to the same Chl *a* concentration (15 µg Chl *a* mL^{-1}). A-

933 Lhcx proteins were detected using a monoclonal anti-FCP6 (Lhcx1). This antibody detects,
934 similarly as the anti-LHCSR of *C. reinhardtii* (Lepetit *et al.*, 2013), also Lhcx2 and Lhcx3 in
935 *P. tricornutum* (strain 'P.t.1') used here as a control. *N. phyllepta* s.l. (N.p.), the dominant
936 species of the MPB community, was also tested. B- and C- Lhcx proteins were detected using
937 a monoclonal anti-Lhcx6 from *T. pseudonana* (T.p.) (Zhu and Green, 2010) which also
938 potentially detect Lhcx3 and an Lhcx dimer in *P. tricornutum* ; C- is a special focus on the
939 band between 33-50 kDa in 37°C exposed samples. Revelation times were: A- 30 s; B- 15 s
940 for the bands between 17-23 kDa, 45 s for the band between 33-50 kDa; C- 30 s;. Note that
941 for A- all samples exposed at 37°C did not yield satisfying signal; and for B-, the sample HL+
942 27°C was lost.

943

944 **Figure 6**

945 **Amount of lipid peroxidation marker (TBARS content in 10^{-6} nmol MDA equivalent**
946 **mL^{-1}) in microphytobenthos harvested at the French site (FR) during light stress**
947 **recovery experiments performed on sediment exposed at two temperatures (27°C, A- or**
948 **37°C, B-) with an inhibitor of cell motility (+Lat A).** Labels as in Fig. 2. Values are mean ±
949 SD (n=6) normalized to surface biomass (I_{diat} biomass index).

950

951 **Figure 7**

952 **Comparison of photoinhibition level (decrease in ΦPSII) and photoprotection (NPQ) in**
953 **microphytobenthos harvested at the Portuguese (PT) and the French (FR) sites during**
954 **light stress recovery experiments performed on sediment exposed at two temperatures**
955 **(27°C or 37°C) and with an inhibitor of cell motility (+Lat A) or without (Ctrl).** ΦPSII

recovery (A) and sustained NPQ (B) after 15 min incubation under LL (50 µmol photons m^{-2} s^{-1}) following 3 h of HL exposure (1200 µmol photons m^{-2} s^{-1}), *** significant difference between sites ($P < 0.001$, Tukey HSD). Values are mean ± SD (n=6).

Figure 8

Western-blot of the Lhcx proteins of microphytobenthos harvested at the Portuguese site during light stress recovery experiments performed on sediment exposed at two temperatures (27°C or 37°C) and with an inhibitor of cell motility (+) or without (-). HL, after 3 h HL (1200 µmol photons. m^{-2}. s^{-1}) treatment; LL, after 3 h of LL exposure. All samples were normalized to the same Chl *a* concentration (15 µg Chl *a* mL^{-1}). Lhcx proteins were detected using a monoclonal anti-FCP6 (Lhcx1). This antibody detects, similarly as the anti-LHCSR of *C. reinhardtii* (Lepetit *et al.*, 2013), also Lhcx2 and Lhcx3 in *P. tricornutum* (strain 'P.t.1') used here as a control. Note that i) the 27°C and 37°C samples were not loaded on the same gel but the revelation time was the same (30 s), ii) the use of the monoclonal anti-Lhcx6 from *T. pseudonana* did not yield any signal with these samples.

Figure 1_Laviale *et al.*

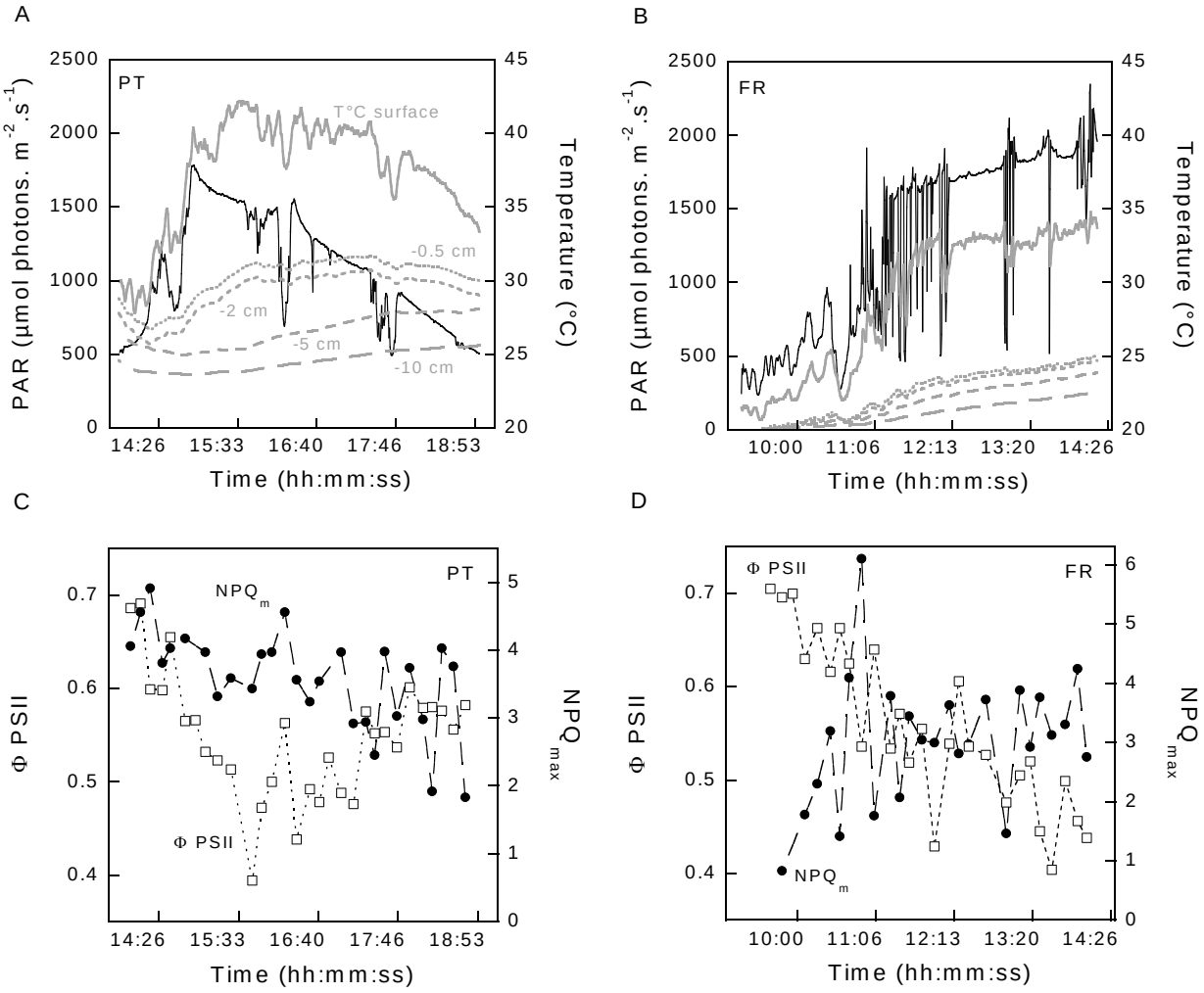

976

977 **Figure 2_Laviale *et al.***

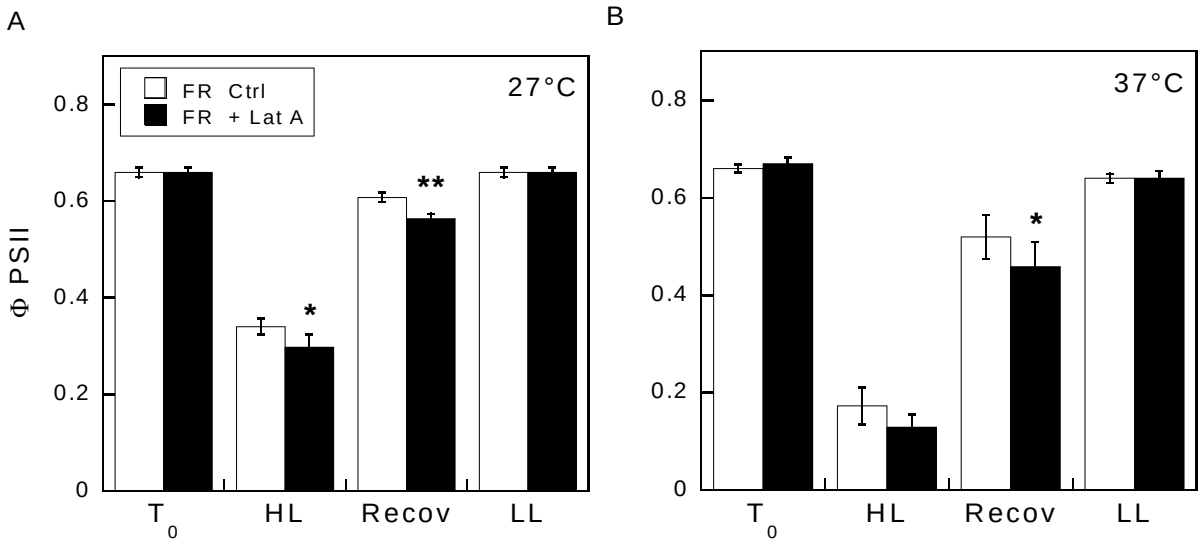

978

979

980

981 **Figure 3_Laviale *et al.***

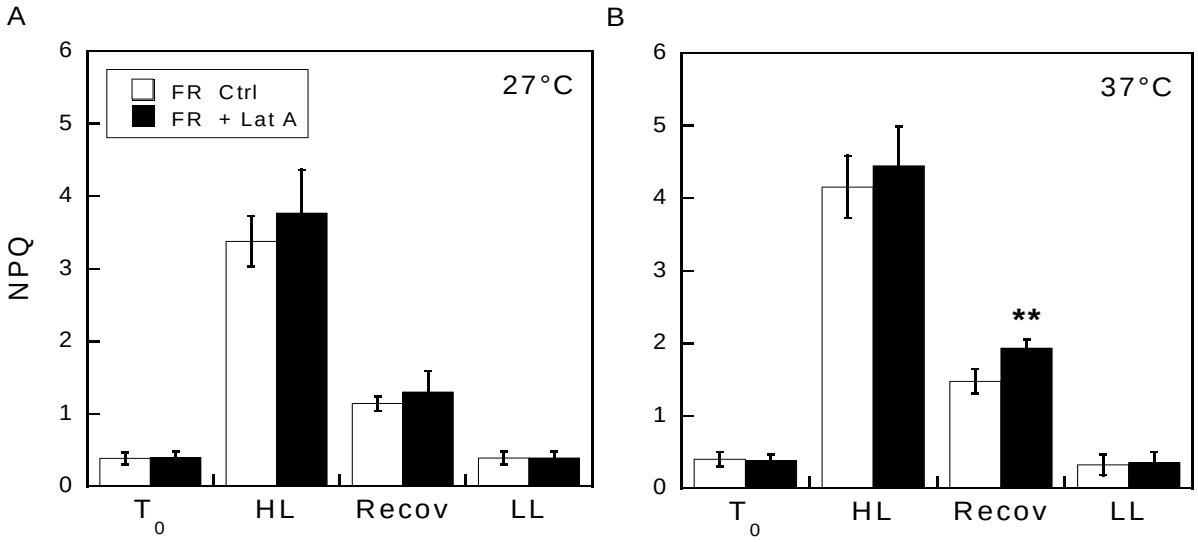

982

983

984

985 **Figure 4_Laviale *et al.***

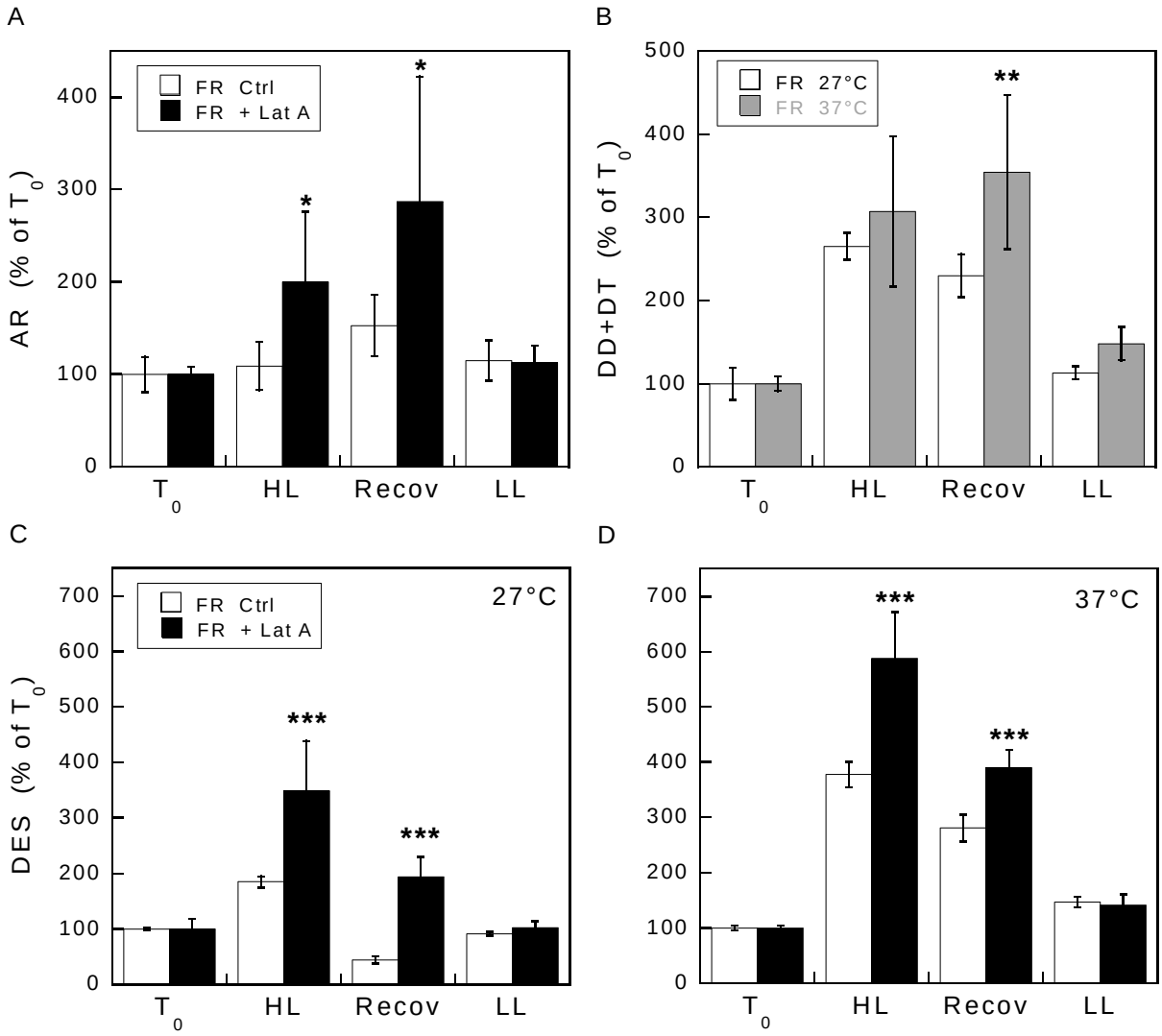

986

987

Figure 5_Laviale *et al.*

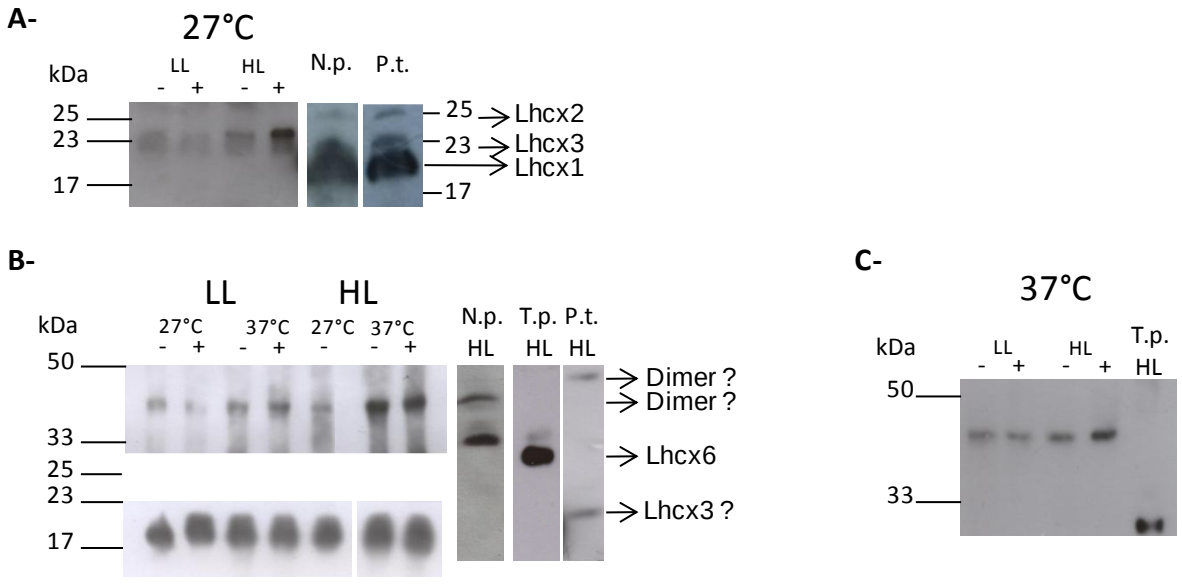

Figure 6_Laviale *et al.*

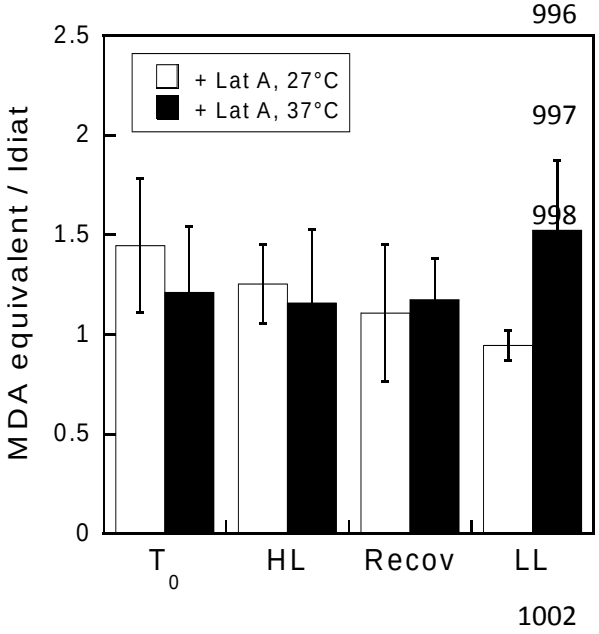

Figure 7_Laviale *et al.*

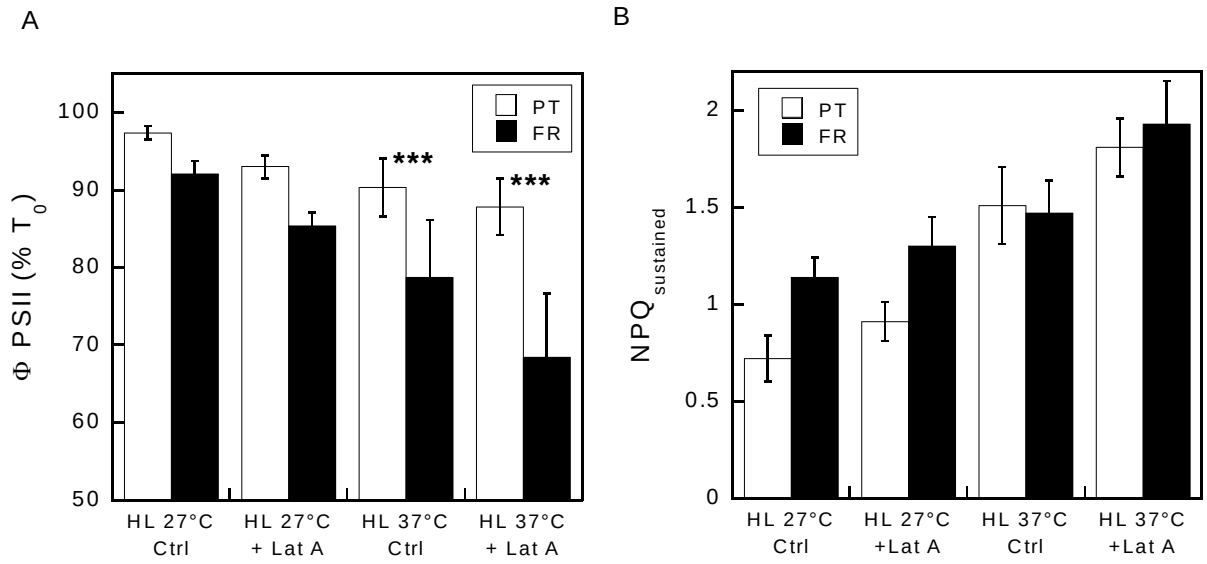

Figure 8_Laviale *et al.*